DOI: 10.61782/fa.2023.0879

forum acusticum 2023

EXTRACTING THE ACOUSTIC-INDUCED VELOCITY WITHIN THE ORIFICE OF A CONVENTIONAL ACOUSTIC LINER: POST-PROCESSING METHODS

Lucas Bonomo[1*] **Francesco Avallone**[2] **Lucas Pereira**[1] **Nicolas Quintino**[1]
Andrey da Silva[1] **Julio Cordioli**[1] **Damiano Casalino**[3]
[1] Federal University of Santa Catarina, Brazil
[2] Politecnico di Torino, Torino, Italy
[3] Delft University of Technology, Delft, The Netherlands

ABSTRACT

Recent developments in aviation towards ultra-high bypass ratio engines are challenging the application of conventional acoustic liner technology. The less space available for their installation is in contrast with the fact that their size would naturally grow due to the lower rotational speed of the fan. However, in order to develop new liner concepts or meta-liner, we must describe the flow-acoustic interaction for conventional liners because this affects their acoustic response. To this end, within the liner orifice, it is essential to decouple the acoustic-induced velocity from the hydrodynamic one in order to understand how the flow affects the acoustic response and vice versa. This is particularly challenging when the liner is grazed by a broadband acoustic source because the simplest approaches based on phase-lock measurements cannot be used. For this reason, in this work, we start comparing results obtained from the triple decomposition, based on a phase-lock approach, with the ones obtained with a wavelet decomposition approach, because the latter can be used for the broadband excitation while the former cannot. We compare the acoustic-induced velocity extracted with the two methods using as input an existing scale-resolved simulation database of a turbulent flow and tonal acoustic excitation grazing a conventional acoustic liner.

Keywords: *acoustic liners, acoustic-induced velocity, grazing flow*

**Corresponding author*: *lucas.bonomo@lva.ufsc.br.*

1. INTRODUCTION

Acoustic liners are passive devices installed at the inlet and bypass walls of turbofan nacelles to reduce fan noise [1]. The simplest liner construction consists of a honeycomb layer topped by a perforated face-sheet and backed by a rigid plate, as shown in Fig. 1. This configuration provides high sound attenuation in a narrow frequency band, typically tuned to match the fundamental blade passing frequency. The frequency tuning is achieved by changing geometrical parameters, such as the perforated plate thickness, hole diameter, percentage of open area, and honeycomb depth [2].

Recent developments in aviation towards ultra-high bypass ratio engines present a challenge for the conventional acoustic liner technology due to the limited space available for their installation. As a matter of fact, the liner thickness must increase to attenuate the lower frequencies of interest for the ultra-high bypass ratio engines due the lower rotational speed of the fan. Therefore novel liners configurations must be developed. However, some of the dominant physical mechanisms for conventional liners are yet not fully understood and must be clearly explained before developing physics-based novel technologies.

A clear example is the case when both a turbulent flow and an acoustic wave graze the acoustic liner. In such

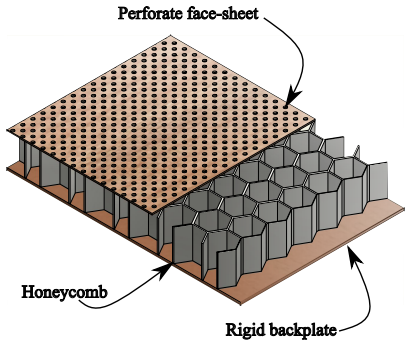

Figure 1: Schematic representation of an acoustic liner.

circumstances, the impedance educed when the acoustic wave propagates in the same direction and in the direction opposite to the mean flow are different, while it is expected to be the same [3]. This has been attributed to the failure of the impedance boundary conditions adopted in the eduction methods, i.e. the Ingard-Myers boundary condition [4]. However, similar discrepancies have been found when performing direct measurement of impedance with the Dean's method [5]. This suggests that there is a change in the physics of the flow-acoustic interaction between the cases where the acoustic wave propagates in the same direction and in the direction opposite to the mean flow, which has not yet described and that may affect the acoustic response of the liner.

To fully understand how the acoustic-flow interaction takes place it is essential to decouple the acoustic-induced velocity from hydrodynamic one caused by the turbulent flow grazing the facesheet. Several methods have been proposed in the literature to separate the acoustic field from the hydrodynamic one, such as triple decomposition [6] and wavelet [7]. However, these methods have not been adopted for the case of interest where the coupling is strong. Furthermore, while the former can be adopted for the case where the acoustic excitation is tonal and the frequency is known, because based on a phase-lock approach, the latter can be further used in the case when the acoustic-excitation is broadband in nature. This case is particularly of interest for future liners where other sources of noise in addition to the fan will be present, i.e. enhanced rotor-stator interaction.

In this work, we make a first attempt to compare two methods: the triple decomposition and formulation $WT1$ proposed by Mancinelli et al. [7]. Results from an existing numerical database, from Pereira et al. [8], are used.

2. HIGH-FIDELITY NUMERICAL MODEL

The numerical results used in this study are taken from Pereira et al. [8]. They were obtained using the commercial lattice-Boltzmann (LB) solver *3DS-Simulia PowerFLOW6-2022R1*, which has been widely adopted to solve fluid dynamic and aeroacoustics problems [9–11].

They investigated the flow over a single degree of freedom acoustic liner with and without grazing flow and tonal plane wave propagating in the same direction and in the direction opposite to the mean flow.

The single degree of freedom liner sample consists of 11 square cavities which are $l = 9.906$ mm (0.39 in) wide. The face sheet of the sample is $\tau = 0.635$ mm (0.025 in) thick and has 8 orifices of diameter $d = 0.9906$ mm (0.039 in) per cavity, which gives a single cavity percentage of open area (POA) equal to 6.3%. The cavities are $h = 38.1$ mm (1.5 in) deep and are completely separated from each other by partition walls $w_p = 2.54$ mm (0.1 in) thick. The streamwise length of tested liner is $L = 136.906$ mm (5.39 in).

The computational domain used is based on the test rig at the Federal University of Santa Catarina (UFSC) [12], as depicted in Fig. 2. The coordinate system is defined at the upstream end of the liner sample, where the z axis is perpendicular to the x and y axes (which are not shown in the figure for clarity). The rectangular cross section of the UFSC test rig is $2H = 40\,\mathrm{mm}$ high in the y direction and $2W = 100\,\mathrm{mm}$ wide in the z direction, which corresponds to a cutoff frequency for plane wave propagation of 3400 Hz [13]. The simulation domain has a width of $W_p = 12.446$ mm and a height of $2H = 40\,\mathrm{mm}$, matching the height of the UFSC test rig. The length of the computational domain extends both upstream and downstream of the liner of a length equal to 10 times the longest acoustic wavelength investigated [8].

Periodic boundary conditions are applied to the boundaries of the domain in the z direction. The orange rectangles represent the channel's inlet and outlet, where a prescribed velocity BC and a static pressure BC are set, respectively. The purple-colored sponge regions are placed at the channel's terminations to prevent reflections of acoustic waves from propagating back towards the sample. The absorbing region is 3λ long, where λ corresponds to the largest wavelength considered in this set of simulations. The gray-colored walls have free-slip BC, and the

blue-colored ones have no-slip BC.

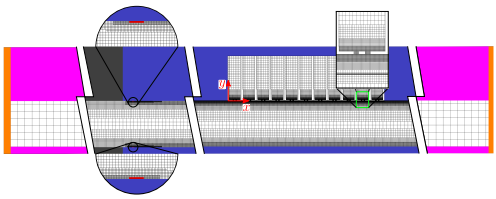

Figure 2: Simulation domain: lattice representation and reference coordinate system.

The boundary layer transition to turbulence is triggered by a tripping geometry located 1.6 m upstream of the liner, aiming at achieving a boundary layer profile as similar as possible to the experimental one.

The lattice refinement scheme is based on the resolution in the liner's orifices, with coarser grid refinement towards the center and the channel's terminations to reduce the computational cost. In this work, only results for resolution of 40 cells per orifice diameter are presented, which were chosen based on previous works involving LBM simulations of acoustic liners [6, 9]. At the moment of the writing of this paper, higher resolution simulations are running to verify convergence.

To perform acoustic simulations, a harmonic acoustic plane wave is superimposed onto the fluid domain. For this purpose, the *Opty∂B* toolkit is used, as previously done by Avallone and Casalino [6]. For converged simulation results, the channel must be long enough to accommodate at least 10 cycles of the lowest frequency considered.

In this paper, only results from 3 simulations of the entire database are reported for the sake of conciseness. The plane acoustic wave has always amplitude equal to 145 dB and frequency equal to 1400 Hz. The 3 cases investigated are: grazing Mach number equal to 0 and plane acoustic wave propagating from upstream of the liner; grazing $M = 0.3$ and grazing acoustic wave propagating from upstream and downstream of the liner sampled, i.e., in the same direction and in the direction opposite to the mean flow.

3. POST-PROCESSING METHODS

3.1 Triple Decomposition

The triple decomposition procedure used in this works follows the one proposed by Avallone and Casalino [6]. The procedure consists of the following steps: (i) since the frequency of the grazing acoustic plane wave is known, phase-lock average of the solution is first performed. The resulting phase-locked velocity components are indicated as $\tilde{u}$, $\tilde{v}$ and $\tilde{w}$. (ii) The time-average of the transient solution is performed and the resulting mean velocity components are indicated as $\bar{u}$, $\bar{v}$ and $\bar{w}$. (iii) The acoustic-induced velocity is then obtained by subtracting the mean velocity field from the phase-locked field, and the acoustic-induced velocity components are indicated as $\bar{\tilde{u}}$, $\bar{\tilde{v}}$ and $\bar{\tilde{w}}$.

3.2 Wavelet Decomposition

Wavelet decomposition has been successfully applied in the separation between hydrodynamic and acoustic components, specially within the near field of a jet source [14]. In this work, we will adopt the *WT3* technique from Mancinelli et al. [7]. The method is based on applying the wavelet transform to the acoustic velocity signals and separating the wavelet coefficients trough a threshold. For our purpose, we mainly want to separate the acoustic-induced velocity from chaotic fluctuations due to the grazing turbulent boundary layer.

The separation algorithm is based on a recursive denoising procedure, where the all the fluctuating components are iteratively evaluated until convergence is obtained. In this work, the *Opty∂B* wavelet tool has been used to this procedure [15]. The threshold level is defined by

$$T_i = \sqrt{2 v_i'^2 \log_2 N_s}, \tag{1}$$

where v_i' is the variance of the acoustic velocity signal counterpart at the i-th iteration and N_s is the number of samples in the signal.

In our application, differently from what done by Mancinelli et al. [7] the acoustic-induced velocity is expected to be related to few but with large amplitude wavelet coefficients. On the other hand, the turbulence-induced velocity, being stochastic in nature, is expected to be represented by many low-amplitude wavelet coefficients.

4. RESULTS

The acoustic-induced velocity and the phase-locked velocity are compared in Fig. 3 (a) and (b), respectively. Data are extracted from the centreline of the central orifice of the most upstream cavity with respect to the direction of propagation of the acoustic wave, i.e. the first

upstream cavity for upstream propagating acoustic wave (when the acoustic wave propagates in the same direction of the mean flow) and the most downstream one when the acoustic wave propagates from downstream (when the acoustic wave propagates in the opposite direction of the mean flow). This is done to ensure that both cavities are exposed to maximum sound pressure level of the acoustic wave.

In agreement with previous studies [16], in absence of a grazing flow ($M = 0$, i..e, continuous line in the figure), the acoustic-induced velocity shows a symmetric behavior between injection (red line) and ejection (blue line) phases. When the grazing flow is present ($M = 0.3$), the phase-locked results show that (i) there is no symmetry between injection and ejection phases and that (ii) there are large differences between the case where the acoustic wave propagates in the same direction and in the direction opposite to the mean flow,i.e. upstream (dashed line) and downstream (dotted line). Furthermore, in presence of grazing flow, it is observed that a non-zero average vertical velocity component is found for both cases.

The non-symmetric behaviour between the injection and ejection phases and the non-zero mean are due to a quasi-steady vortex that is formed within the orifice, also in absence of grazing acoustic wave, because of the convecting turbulent boundary layer, as shown in previous studies [6, 8].

By applying the triple decomposition, the symmetry between the injection and ejection phase is mostly recovered for both upstream and downstream propagating acoustic wave and, therefore, the mean between the two phases is zero. Furthermore, it is found that the maximum acoustic-induced velocity in presence of grazing flow is approximately equal to the maximum acoustic-induced velocity in absence of grazing flow ($M = 0$).

By comparing the cases with and without grazing flow, it can be concluded that the effect of the quasi-steady vortex in the cavity is to reduce the effective area of the orifice itself. This results in an increase of resistance, i.e. the real part of the impedance, the quantity measured to characterize the acoustic response of a liner. Even if not reported here, for the sake of conciseness, this is consistent with both experimental measurements and simulation results [8]. Similarly, it can be argued that there is a difference in acoustic response between the two cases with acoustic wave propagating in the same direction and opposite to the mean flow direction. A similar dependence on the impedance, as described above, is found also in this case when looking at the numerically measured impedance.

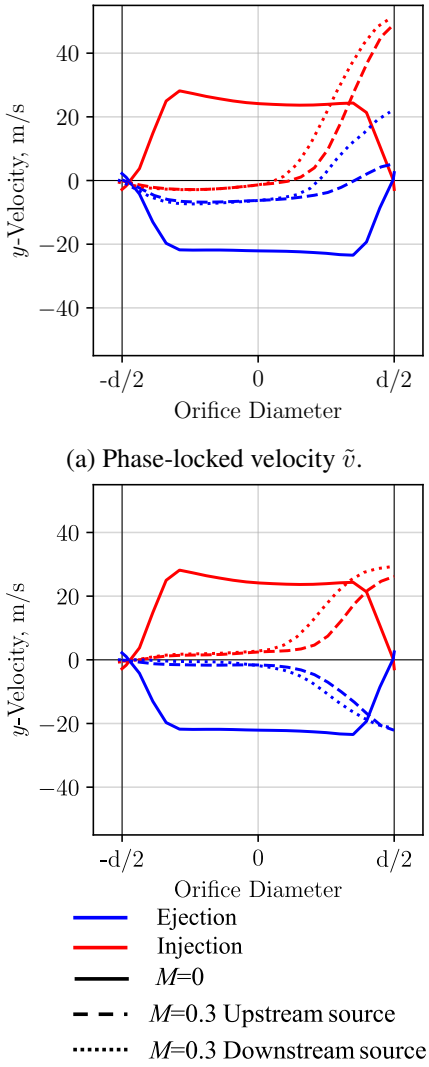

(a) Phase-locked velocity $\tilde{v}$.

(b) Acoustic-induced velocity $\bar{\bar{v}}$.

Figure 3: Comparison between phase-lock results and triple decomposition for the three cases investigated.

In Fig. 4 the comparison of the acoustic-induced velocity obtained with the triple decomposition and the wavelet one is reported. A perfect agreement is observed for the results in the absence of flow, while a reasonable agreement is observed for the cases in the presence of a grazing flow. The only difference is found for the ejection phase where a discrepancy exists between the two meth-

ods. However, it can be observed that the wavelet decomposition, differently from the triple decomposition, shows almost a perfect symmetry between the injection and ejection phase. This might indicate that the wavelet decomposition can be more reliable than the triple decomposition one for the case of interest where the transient signal is short because of computational cost. Additional analysis are needed to verify this statement.

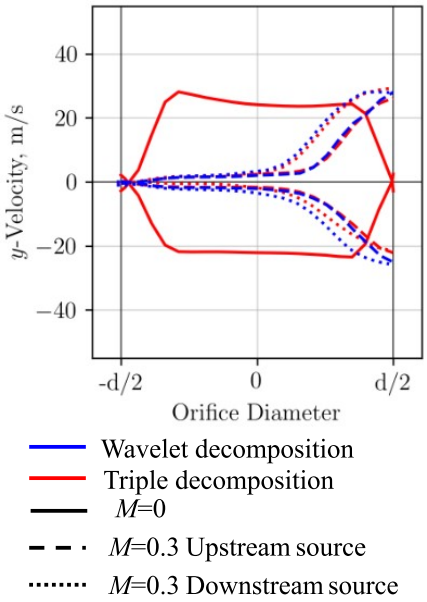

Figure 4: In-orifice velocity profiles from the maximum and minimum value phases, induced by a 1400 Hz acoustic excitation at 145 dB. Comparison of the results obtained with the triple decomposition and wavelet decomposition methods.

5. CONCLUDING REMARKS AND FUTURE WORK

In this paper a first attempt to compare to methods to separate the acoustic-induced velocity from the hydrodynamic one in a liner orifice is presented. Data from an existing high-fidelity numerical database have been used. At today, two methods are compared: the triple decomposition and the wavelet decomposition. The two methods show, as expected for the case tested, a reasonable agreement with the wavelet decomposition being able to obtain, based on expectations, slightly better results for the ejection phase.

The next steps in the research is to extends the comparisons using the method $WT1$ reported by Mancinelli et al. [7] and apply to the case where the acoustic excitation is of broadband nature and the simplest approach as the triple decomposition cannot be used.

6. ACKNOWLEDGMENTS

This study was financed in part by the Coordenação de Aperfeiçoamento de Pessoal de Nível Superior – Brasil (CAPES) – Finance Code 001. The Aeroacoustics Research Consortium (AARC) supports this work, as well as the Brazilian research agencies CNPq and FINEP. The work of Francesco Avallone is supported also by the ERC Starting Grant project LINING (grant agreement 101075903). The authors acknowledge PRACE for awarding us access to Prometheus at PSNC@CYFRONET, Poland. The authors gratefully acknowledge the support from Davide Cerizza (3DS).

7. REFERENCES

[1] M. J. T. Smith, *Aircraft Noise*. Cambridge Aerospace Series, Cambridge University Press, 1989.

[2] A. W. Guess, "Calculation of perforated plate liner parameters from specified acoustic resistance and reactance," *Journal of Sound and Vibration*, vol. 40, pp. 119–137, 5 1975.

[3] Y. Renou and Y. Aurégan, "Failure of the ingard–myers boundary condition for a lined duct: An experimental investigation," *The Journal of the Acoustical Society of America*, vol. 130, pp. 52–60, 7 2011.

[4] M. Myers, "On the acoustic boundary condition in the presence of flow," *Journal of Sound and Vibration*, vol. 71, no. 3, pp. 429–434, 1980.

[5] P. D. Dean, "An in situ method of wall acoustic impedance measurement in flow ducts," *Journal of Sound and Vibration*, vol. 34, pp. 97–IN6, 5 1974.

[6] F. Avallone and D. Casalino, "Acoustic-induced velocity in a multi-orifice acoustic liner grazed by a turbulent boundary layer," *AIAA Aviation Forum*, 2021.

[7] M. Mancinelli, T. Pagliaroli, A. Di Marco, R. Camussi, and T. Castelain, "Wavelet decomposition of hydrodynamic and acoustic pressures in the near field of the jet," *Journal of Fluid Mechanics*, vol. 813, pp. 716–749, 2017.

[8] L. M. Pereira, L. A. Bonomo, N. T. Quintino, A. R. da Silva, J. A. Cordioli, and F. Avallone, "Validation of high-fidelity numerical simulations of acoustic liners under grazing flow," in *2023 AIAA Aviation Forum*, 2023.

[9] P. Manjunath, F. Avallone, D. Casalino, D. Ragni, and M. Snellen, "Characterization of liners using a lattice-boltzmann solver," *2018 AIAA/CEAS Aeroacoustics Conference*, 2018.

[10] D. Casalino, A. Hazir, and A. Mann, "Turbofan broadband noise prediction using the lattice boltzmann method," *AIAA Journal*, vol. 56, pp. 609–628, 2018.

[11] M. Bauerheim and L. Joly, "Les of the aero-acoustic coupling in acoustic liners containing multiple cavities," *AIAA Aviation Forum*, 2020.

[12] L. A. Bonomo, N. T. Quintino, A. Spillere, J. A. Cordioli, and P. B. Murray, "A comparison of in-situ and impedance eduction experimental techniques for acoustic liners with grazing flow and high spl," *28th AIAA/CEAS Aeroacoustics 2022 Conference*, 2022.

[13] A. M. N. Spillere, L. A. Bonomo, J. A. Cordioli, and E. J. Brambley, "Experimentally testing impedance boundary conditions for acoustic liners with flow: Beyond upstream and downstream," *Journal of Sound and Vibration*, vol. 489, 12 2020.

[14] R. Camussi and S. Meloni, "On the application of wavelet transform in jet aeroacoustics," *Fluids 2021, Vol. 6, Page 299*, vol. 6, p. 299, 8 2021.

[15] W. van der Velden, D. Casalino, P. Gopalakrishnan, A. Jammalamadaka, Y. Li, R. Zhang, and H. Chen, "Validation of jet noise simulations and resulting insights of acoustic near field," *AIAA Journal*, vol. 57, no. 12, pp. 5156–5167, 2019.

[16] Q. Zhang and D. J. Bodony, "Numerical investigation and modelling of acoustically excited flow through a circular orifice backed by a hexagonal cavity," *Journal of Fluid Mechanics*, vol. 693, p. 367–401, 2012.